sciendo Applied Mathematics and Nonlinear Sciences 6(1) (2021) 403–420

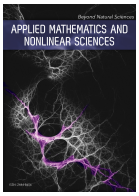

Applied Mathematics and Nonlinear Sciences

https://www.sciendo.com

Two equal collinear cracks in magneto-electro-elastic materials: A study of electric and magnetic poling influences

Kamlesh Jangid

Department of Mathematics, Rajasthan Technical University Kota, India 324010,
E-mail: jangidkamlesh7@gmail.com

Submission Info

Communicated by Jagdev Singh
Received August 22nd 2020
Accepted January 4th 2020
Available online June 26th 2020

Abstract

In this paper, the problem of two equal collinear cracks is analytically studied for two-dimensional (2D) arbitrarily polarized magneto-electro-elastic materials. The electric and magnetic poling directions make arbitrary angles with the crack line. The Stroh's formalism and complex variable methodology is utilized to reduce the problem into non-homogeneous Riemann Hilbert problem. This numerical problem is then comprehended with the Riemann Hilbert way to obtain the intensity factors for stress, electric displacement and magnetic induction. A numerical contextual analysis is displayed for the $BaTiO_3 - CoFe_2O_4$ composite. The numerical examination demonstrates that the change in electric/magnetic poling directions influences the intensity factors.

Keywords: complex variable; collinear cracks; piezomagnetic/piezoelectric composite; poling directions; Riemann-Hilbert problem.

1 Introduction

Magneto-electro-elastic(MEE) composite materials prepared by combining the ferrite and ferroelectric materials. The coupling interaction among ferroelectric and ferrite produces an interesting effect which has drawn the enthusiasm of scientists. MEE composites have a wide scope of utilization in electronics industries. Ferrite鈥攇erroelectric composites could create both piezomagnetic and piezoelectric effects. Use of a magnetic field could incite electric polarization and an electric field could instigate magnetization. This is because of the strain or mechanical deformation caused by the ferrite and ferroelectric phase of the composite.

It is well-known that a wide range of poled MEE materials retains their aligned electric and magnetic dipole fields in the material microstructure below Curie temperature. Alignment of poling directions of piezomagnetic and piezoelectric materials can add to the complexity of the MEE material behavior to which this study will be concerned with. Various investigations have demonstrated that the electric/magnetic poling directions incredibly impact crack growth in piezoelectric/MEE media [1–8].

sciendo ISSN 2444-8656 doi:10.2478/AMNS.2020.2.00009 sciendo

In analogous to the piezoelectric materials, Sih et al. [7] explore the piezomagnetic and piezoelectric poling influence on mode I and II crack initiation behavior of MEE materials. They found that the alignment of the poling directions of piezomagnetic and piezoelectric materials influences the various fracture parameters. Sih and Song [8] demonstrated that the poling directions presented magnetically and electrically could be different notwithstanding those for the applied magnetic and electric field. Their choices could influence the character of crack growth which could be enhanced or retarded. In the proposed model [8] they found that crack growth in the MEE materials could be stifled by expanding the magnitude of the piezomagnetic constants about those for piezoelectricity. Song and Sih [9] investigated the crack initiation behavior in MEE composite under in-plane deformation. They found that the magnetostrictive effect could have an influence on crack initiation as the prescribed field directions changed.

The earlier research work on the fracture in MEE materials was mainly on single crack, while in this paper we have investigated the problem for two collinear cracks in MEE media.

Considering the significance of the electric poling and magnetic poling in MEE materials, we propose and investigate the influence of the electric/magnetic poling on two equal collinear cracks in MEE media.

NOMENCLATURE

Symbol	**Notation**
d	inner crack tip
c	outer crack tip
e_{iks}	piezoelectric constants
f	analytic function
h_{iks}	piezomagnetic constants
k_1	elliptic modulus
$\mathbf{m}_E$	coordinate transfer matrix of electric poling
$\mathbf{m}_H$	coordinate transfer matrix of magnetic poling
$\mathbf{u}$	generalized displacement vector
$u_i\ (i=1,2,3)$	mechanical displacement
$x_i\ (i=1,2,3)$	material coordinate system
z	complex variable
C_{ijks}	elastic constants
$E(k_1)$	complete elliptic integral of second kind
$F(k_1)$	complete elliptic integral of first kind
$\mathbf{M}^B$	material constants transform matrix of the inclusion
$\mathbf{M}^C$	material constants transform matrix of the matrix
V_f	volume fraction of the inclusion
α_{is}	dielectric permittivities
β_{is}	electromagnetic constants
γ_{is}	magnetic permeabilities
$u_4=\phi$	electric potential
$u_5=\varphi$	magnetic potential
χ	Jacobi amplitude

2 General equations

In-rectangular Cartesian coordinate system $x_i(i=1,2,3)$ the stress ,σ_{ij}, electric displacement ,D_i, and magnetic induction ,B_i, are linearly related to the strain ,ε_{ij}, electric field ,E_i, and magnetic field ,H_i,. A set of

constitutive equations for a MEE material would thus be able to be written in the form:

$$\begin{aligned} \sigma_{ij} &= C_{ijks}\varepsilon_{ks} - e_{sij}E_s - h_{sij}H_s \\ D_i &= e_{iks}\varepsilon_{ks} + \alpha_{is}E_s + \beta_{is}H_s \\ B_i &= h_{iks}\varepsilon_{ks} + \beta_{is}E_s + \gamma_{is}H_s \end{aligned} \tag{1}$$

The conditions of equilibrium in the absence of body forces are given by

$$\sigma_{ij,j} = 0, \qquad D_{i,i} = 0, \qquad B_{i,i} = 0. \tag{2}$$

For linear problems, the accompanying relations can be utilized:

$$\varepsilon_{ij} = \frac{1}{2}\left(u_{i,j} + u_{j,i}\right), \qquad E_i = -\phi_{,i}, \qquad H_i = -\varphi_{,i} \tag{3}$$

3 In-plane extension and solution methodology

For a transversely isotropic MEE materials, the constitutive relations in the ox_1x_3-plane under plane strain (i.e., $D_2 = B_2 = 0$, $\sigma_{12} = \sigma_{23} = 0$) are given in Song and Sih [8].

Let the magnetic poling H and electric poling E are oriented arbitrarily with the x_1-axis by the respective angles of θ_H and θ_E. In this case, the constants C_{ijks}, e_{iks}, h_{iks}, α_{is} and γ_{is} referred to the x_1x_3 (or xy)-coordinate system are given in *Appendix A*.

To find the generalized 2D deformations, the generalized displacement vector $\mathbf{u}$ depending on two independent variables x_1 and x_3 (or x and y) are considered as follows:

$$\mathbf{u} = (u_1, u_3, \phi, \varphi)^T = \mathbf{a}f(x_1 + px_3) \tag{4}$$

Since $\mathbf{u}$ is the generalized 2D solution of the problem, it must satisfy the field Eqs.(1), (2), (3) and given by:

$$\begin{pmatrix} c_{11}+c_{44}p^2 & (c_{13}+c_{44})p & (e_{31}+e_{15})p & (h_{31}+h_{15})p \\ (c_{13}+c_{44})p & c_{44}+c_{33}p^2 & e_{15}+e_{33}p^2 & h_{15}+h_{33}p^2 \\ (e_{31}+e_{15})p & e_{15}+e_{33}p^2 & -(\alpha_{11}+\alpha_{33}p^2) & 0 \\ (h_{31}+h_{15})p & h_{15}+h_{33}p^2 & 0 & -(\gamma_{11}+\gamma_{33}p^2) \end{pmatrix} \mathbf{a} = \mathbf{0}. \tag{5}$$

This is an eigenvalue problem consisting of four equations; a non-trivial $\mathbf{a}$ exists if p is a root of the determinant polynomial

$$\det\left(\begin{pmatrix} c_{11}+c_{44}p^2 & (c_{13}+c_{44})p & (e_{31}+e_{15})p & (h_{31}+h_{15})p \\ (c_{13}+c_{44})p & c_{44}+c_{33}p^2 & e_{15}+e_{33}p^2 & h_{15}+h_{33}p^2 \\ (e_{31}+e_{15})p & e_{15}+e_{33}p^2 & -(\alpha_{11}+\alpha_{33}p^2) & 0 \\ (h_{31}+h_{15})p & h_{15}+h_{33}p^2 & 0 & -(\gamma_{11}+\gamma_{33}p^2) \end{pmatrix}\right) = 0 \tag{6}$$

Note that p are the eigenvalues. Only the four roots of p in upper half complex plane are considered such that the general solution (according to Stroh's formalism [11] and Jangid [10]) is given by:

$$\mathbf{u}_{,1} = \mathbf{A}\mathbf{F}(z) + \overline{\mathbf{A}\mathbf{F}(z)} \tag{7}$$

$$\blacksquare_{,1} = \mathbf{B}\mathbf{F}(z) + \overline{\mathbf{B}\mathbf{F}(z)} \tag{8}$$

where $\mathbf{A} = (\mathbf{a}_1, \mathbf{a}_2, \mathbf{a}_3, \mathbf{a}_4)$, $\mathbf{B} = (\mathbf{b}_1, \mathbf{b}_2, \mathbf{b}_3, \mathbf{b}_4)$, $\mathbf{F}(z) = d\mathbf{f}(z)/dz$,
$\mathbf{f}(z_\alpha) = [f_1(z_1), f_2(z_2), f_3(z_3), f_4(z_4)]^T$, $z_\alpha = x_1 + p_\alpha x_3$.

and $\blacksquare$ is the generalized stress function such that

$$\sigma_1 = (\sigma_{11}, \sigma_{13}, D_1, B_1)^T = -\blacksquare_{,\mathbf{3}} \tag{9}$$

$$\sigma_3 = (\sigma_{31}, \sigma_{33}, D_3, B_3)^T = \blacksquare_{,\mathbf{1}} \tag{10}$$

4 Statement of the problem

An infinitely transversely isotropic MEE plate occupying the x_1x_3-plane is considered. The magnetic and electric poling are arbitrarily oriented with the crack line and make the respective angles of θ_H and θ_E. The plate is cut with two equal collinear cracks symmetrically situated about the origin and occupying the intervals $[-c,-d]$ and $[d,c]$ along the x_1-axis. The plate is subjected to under the effect of the remote uniform tensile, in-plane electric displacement and magnetic induction loadings, i.e., $\sigma_{33}=\sigma_{33}^{\infty}$, $D_3=D_3^{\infty}$ and $B_3=B_3^{\infty}$. The entire configuration of the problem is schematically presented in Fig.1.

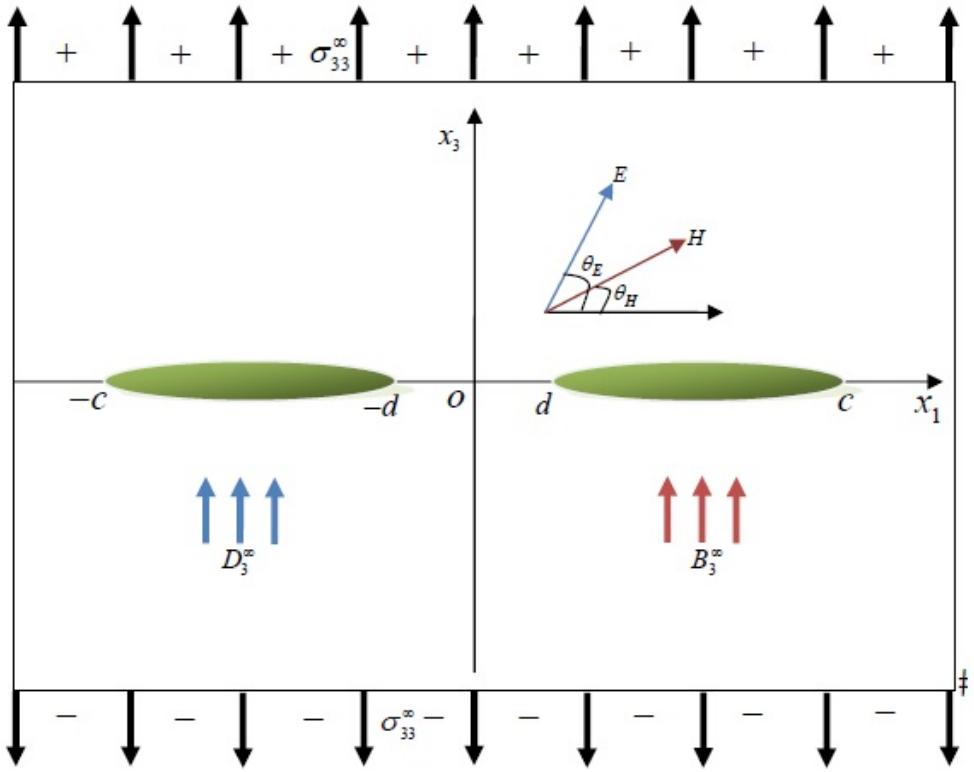

Fig. 1 Schematic representation of the problem

The physical boundary conditions of the problem can be mathematically written as follows:

(i) $\sigma_{3j}^{+}=\sigma_{3j}^{-}, D_3^{+}=D_3^{-}=0, B_3^{+}=B_3^{-}=0, \blacksquare_{,1}^{+}=\blacksquare_{,1}^{-}=-(0,\sigma_{33}^{\infty},D_3^{\infty},B_3^{\infty})^T, d<|x_1|<c,$

(ii) $\sigma_{33}=\sigma_{33}^{\infty},\ \ D_3=D_3^{\infty},\ \ B_3=B_3^{\infty},\qquad |x_3|\to\infty$

(iii) $u_j^{+}=u_j^{-},\ \sigma_{3j}^{+}=\sigma_{3j}^{-}, D_3^{+}=D_3^{-},\ B_3^{+}=B_3^{-},\quad |x_1|>c$

5 Solution of the problem

The continuity of $\blacksquare_{,1}$ on x_1-axis yield

$$\left[\mathbf{BF}(x_1)-\overline{\mathbf{BF}(x_1)}\right]^{+}-\left[\mathbf{BF}(x_1)-\overline{\mathbf{BF}(x_1)}\right]^{-}=\mathbf{0} \tag{11}$$

Following Muskhelishvili [12], the solution of Eq.(11) can be written as

$$\mathbf{BF}(z) = \overline{\mathbf{BF}(z)} = \mathbf{h}(z) \text{ (say)} \tag{12}$$

Using boundary condition (i) into the Eqs.(8), (12), we get

$$\mathbf{h}^{+}(x_1) + \mathbf{h}^{-}(x_1) = -(0, \sigma_{33}^{\infty}, D_3^{\infty}, B_3^{\infty})^T \tag{13}$$

Introducing a new complex function vector as

$$\blacksquare(z) = [\Omega_1(z), \Omega_2(z), \Omega_3(z), \Omega_4(z)]^T = \mathbf{HBF}(z)$$

such that $\mathbf{h}(z) = \blacksquare\blacksquare(z)$, $\blacksquare = \mathbf{H}^{-1}$, $\mathbf{H} = 2Re(\mathbf{Y})$ and $\mathbf{Y} = i\mathbf{AB}^{-1}$.

Eq.(13) can be written in its components $\Omega_2(z)$, $\Omega_3(z)$ and $\Omega_4(z)$ as follows:

$$\Upsilon_{22}\left[\Omega_2^{+}(x_1) + \Omega_2^{-}(x_1)\right] + \Upsilon_{23}\left[\Omega_3^{+}(x_1) + \Omega_3^{-}(x_1)\right] + \Upsilon_{24}\left[\Omega_4^{+}(x_1) + \Omega_4^{-}(x_1)\right] = -\sigma_{33}^{\infty} \tag{14}$$

$$\Upsilon_{32}\left[\Omega_2^{+}(x_1) + \Omega_2^{-}(x_1)\right] + \Upsilon_{33}\left[\Omega_3^{+}(x_1) + \Omega_3^{-}(x_1)\right] + \Upsilon_{34}\left[\Omega_4^{+}(x_1) + \Omega_4^{-}(x_1)\right] = -D_3^{\infty} \tag{15}$$

$$\Upsilon_{42}\left[\Omega_2^{+}(x_1) + \Omega_2^{-}(x_1)\right] + \Upsilon_{43}\left[\Omega_3^{+}(x_1) + \Omega_3^{-}(x_1)\right] + \Upsilon_{44}\left[\Omega_4^{+}(x_1) + \Omega_4^{-}(x_1)\right] = -B_3^{\infty} \tag{16}$$

Following Muskhelishvili [12], the solution of above equations can be written as:

$$\Omega_2(z) = \frac{\Pi_1}{2\Pi}\left\{\frac{z^2 - c^2\lambda_1^2}{X(z)} - 1\right\} \tag{17}$$

$$\Omega_3(z) = \frac{\Pi_2}{2\Pi}\left\{1 - \frac{z^2 - c^2\lambda_1^2}{X(z)}\right\} \tag{18}$$

$$\Omega_4(z) = \frac{\Pi_3}{2\Pi}\left\{1 - \frac{z^2 - c^2\lambda_1^2}{X(z)}\right\} \tag{19}$$

where $X(z) = \sqrt{(z^2 - d^2)(z^2 - c^2)}$, $\lambda_1^2 = E(k_1)/F(k_1)$, $k_1^2 = (c^2 - d^2)/c^2$. Π, Π_1, Π_2 and Π_3 are given in *Appendix B*.

6 Derivation of the fracture parameters

In this section, the explicit expressions are determined for the stress, electric displacement, and magnetic induction intensity factors.

6.1 Stress intensity factor(SIF)

Open mode stress intensity factor, K_I, at the crack tips $x_1 = d$ and $x_1 = c$, may be calculated using the following formulae

$$K_I(d) = \lim_{x_1 \to d^-} \sqrt{2\pi(d - x_1)}\sigma_{33}(x_1), \tag{20}$$

$$K_I(c) = \lim_{x_1 \to c^+} \sqrt{2\pi(x_1 - c)}\sigma_{33}(x_1). \tag{21}$$

Substituting $\sigma_{33}(x_1)$ obtained from Eqs.(8, 17, 18 and 19) into above equations and simplifying one obtains

$$K_I(d) = -\sqrt{\frac{\pi}{d(c^2 - d^2)}}(d^2 - c^2\lambda_1^2)\left(\frac{\Upsilon_{22}\Pi_1 - \Upsilon_{23}\Pi_2 - \Upsilon_{24}\Pi_3}{\Pi}\right), \tag{22}$$

$$K_I(c) = \sqrt{\frac{\pi}{c(c^2 - d^2)}}(c^2 - c^2\lambda_1^2)\left(\frac{\Upsilon_{22}\Pi_1 - \Upsilon_{23}\Pi_2 - \Upsilon_{24}\Pi_3}{\Pi}\right). \tag{23}$$

6.2 Electric displacement intensity factor(EDIF)

The EDIF, K_{IV}, at the crack tips $x_1 = d$ and $x_1 = c$, may be calculated using the following formulae

$$K_{IV}(d) = -\sqrt{\frac{\pi}{d(c^2-d^2)}}(d^2 - c^2\lambda_1^2)\left(\frac{\Upsilon_{32}\Pi_1 - \Upsilon_{33}\Pi_2 - \Upsilon_{34}\Pi_3}{\Pi}\right), \tag{24}$$

$$K_{IV}(c) = \sqrt{\frac{\pi}{c(c^2-d^2)}}(c^2 - c^2\lambda_1^2)\left(\frac{\Upsilon_{32}\Pi_1 - \Upsilon_{33}\Pi_2 - \Upsilon_{34}\Pi_3}{\Pi}\right). \tag{25}$$

6.3 Magnetic induction intensity factor(MIIF)

Analogous to SIF and EDIF, the MIIF, K_V, at the crack tips $x_1 = d$ and $x_1 = c$, may be calculated using the following formulae

$$K_V(d) = -\sqrt{\frac{\pi}{d(c^2-d^2)}}(d^2 - c^2\lambda_1^2)\left(\frac{\Upsilon_{42}\Pi_1 - \Upsilon_{43}\Pi_2 - \Upsilon_{44}\Pi_3}{\Pi}\right), \tag{26}$$

$$K_V(c) = \sqrt{\frac{\pi}{c(c^2-d^2)}}(c^2 - c^2\lambda_1^2)\left(\frac{\Upsilon_{42}\Pi_1 - \Upsilon_{43}\Pi_2 - \Upsilon_{44}\Pi_3}{\Pi}\right). \tag{27}$$

7 Numerical results and discussion

In this section, numerical study for arbitrarily polarized MEE composite is presented. A problem of two equal collinear semi-permeable cracks in a 2D infinite $BaTiO_3 - CoFe_2O_4$ plate is considered. The plate is infinite in the sense that the length of the crack is small as compared to the plate. For the whole numerical study, the length of the crack and volume fraction V_f of the inclusion $BaTiO_3$ are taken fixed as $10mm$ and 0.5, respectively, unless otherwise stated. The plate is subjected to the far-field loadings with the mechanical loading, $\sigma_{33}^{\infty} = 5MPa$, electric displacement, $D_3^{\infty} = 2(e_{33}/c_{33})\sigma_{33}^{\infty}$, and magnetic induction $B_3^{\infty} = 2(h_{33}/c_{33})\sigma_{33}^{\infty}$. The behaviors of the fracture parameters obtained in section 6 are demonstrated graphically with electric and magnetic poling directions. The material constants of the $BaTiO_3 - CoFe_2O_4$ taken for the study are taken from Jangid [10].

In the first analysis, the effect of electric poling direction is shown on the various fracture parameters such as SIF, EDIF, and MIIF with fixed magnetic poling direction (such as $\theta_H = 0^0, 30^0, 90^0$).

7.1 Effect of electric poling direction

Figs. (2,3,4), Figs. (5,6,7) and Figs. (8,9,10), respectively, represent the behaviors of SIF, EDIF and MIIF versus inter-crack distance for different θ_E with fixed θ_H. It is observed that the values of K_I, K_{IV} and K_V increases as θ_E increased. Also, the values of K_I, K_{IV} and K_V at the inner crack tip $x_1 = d$ are higher than that at outer tip $x_1 = c$, because of the mutual interaction of the two collinear cracks on the inner crack tips. And the values of K_I, K_{IV} and K_V at both the crack tips get coincide as the inter-crack distance increases. Moreover, the effect of θ_E is negligible over K_I in Figs. (2,3) for $\theta_H = 0^0$ and 30^0.

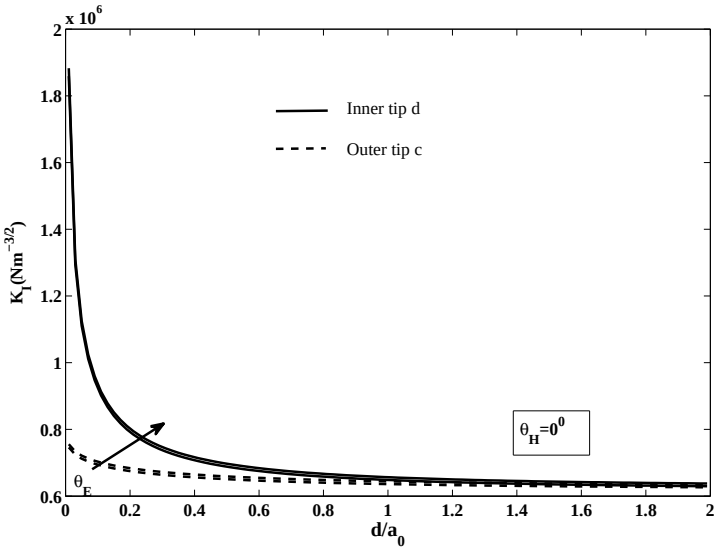

Fig. 2 SIF versus inter-crack distance for different electric poling with fixed magnetic poling

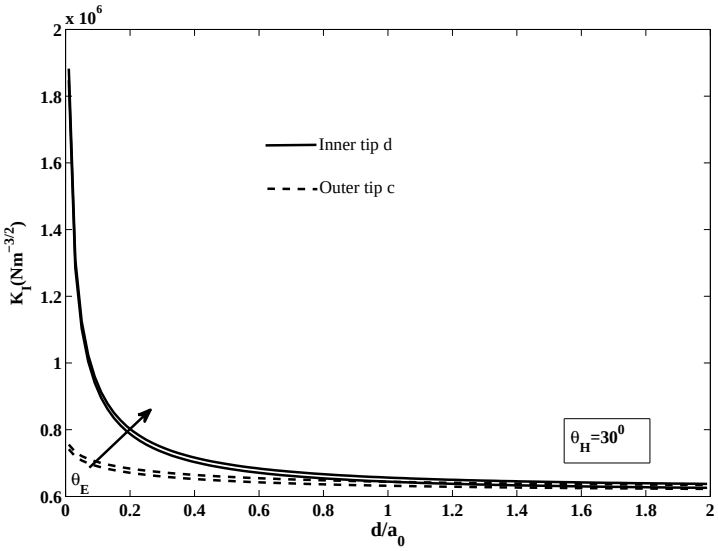

Fig. 3 SIF versus inter-crack distance for different electric poling with fixed magnetic poling

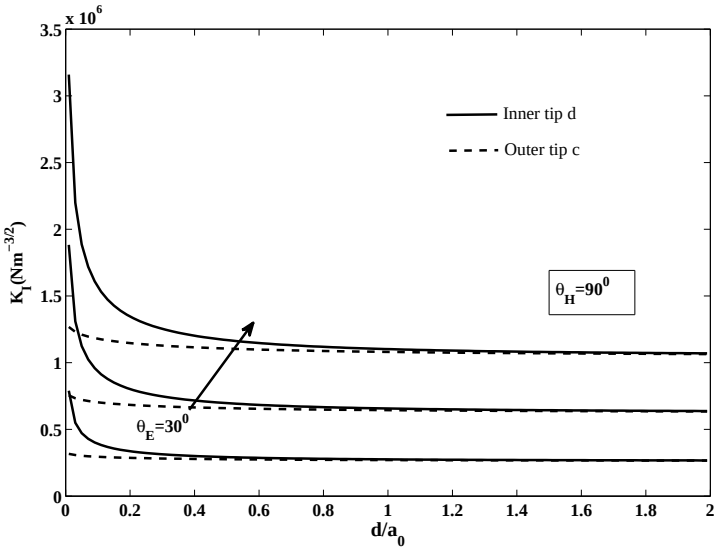

Fig. 4 SIF versus inter-crack distance for different electric poling with fixed magnetic poling

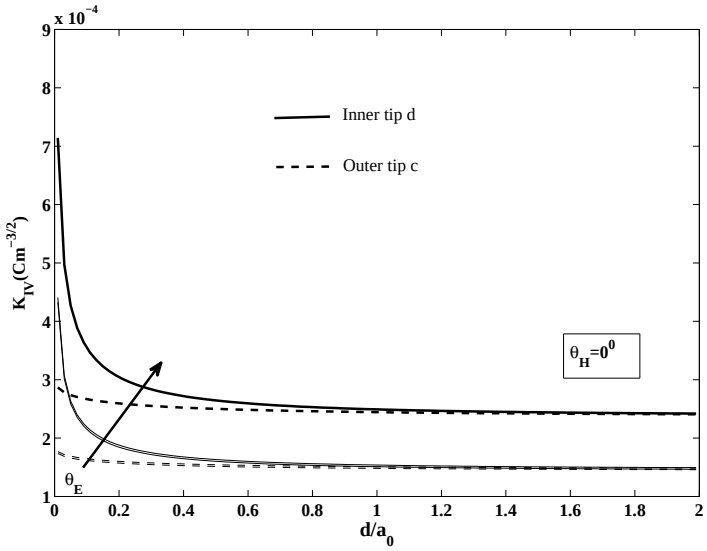

Fig. 5 EDIF versus inter-crack distance for different electric poling with fixed magnetic poling

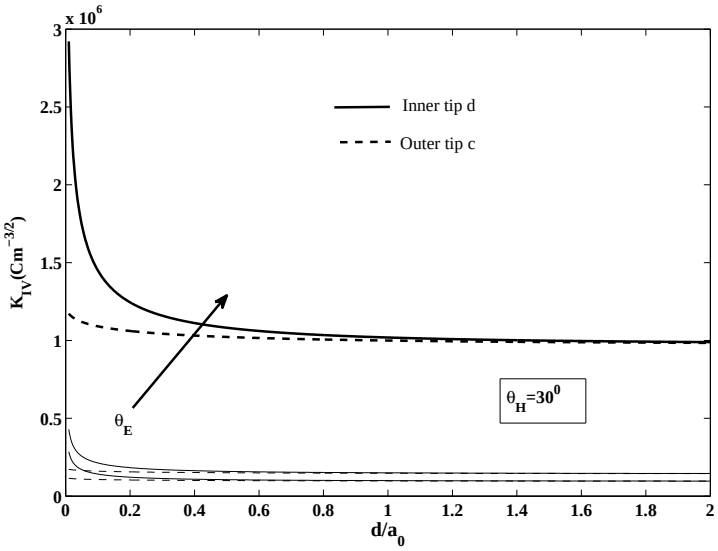

Fig. 6 EDIF versus inter-crack distance for different electric poling with fixed magnetic poling

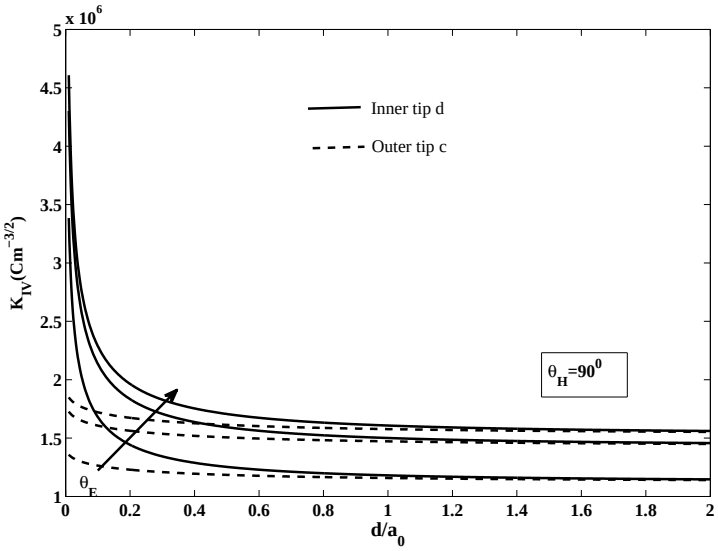

Fig. 7 EDIF versus inter-crack distance for different electric poling with fixed magnetic poling

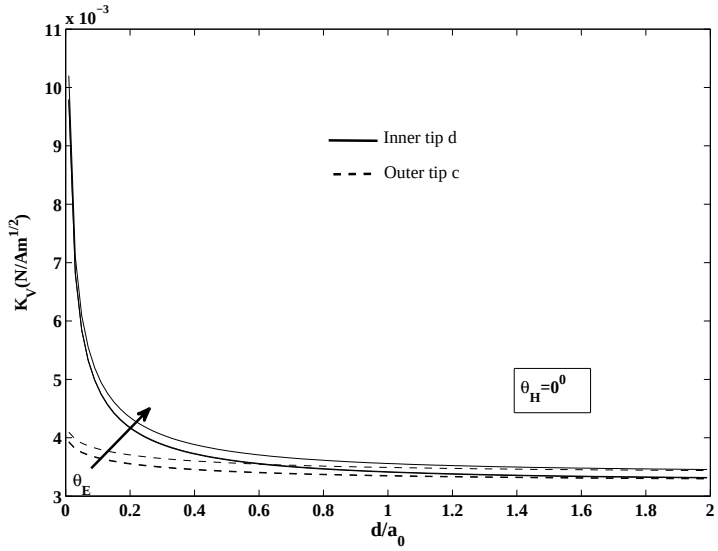

Fig. 8 MIIF versus inter-crack distance for different electric poling with fixed magnetic poling

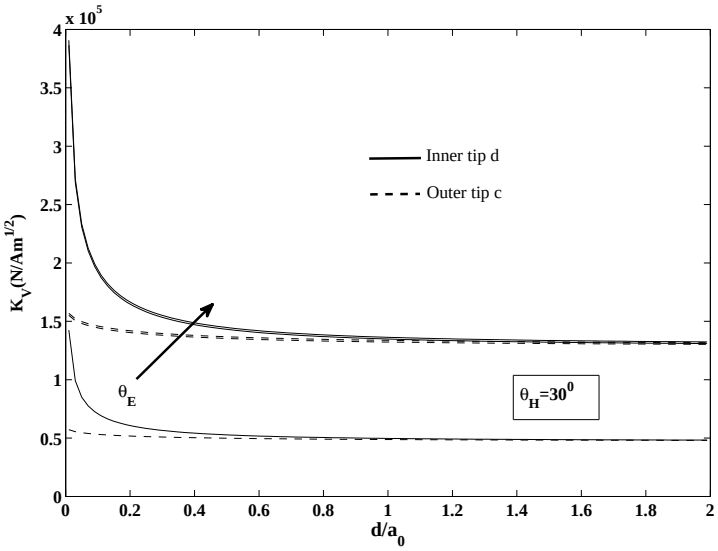

Fig. 9 MIIF versus inter-crack distance for different electric poling with fixed magnetic poling

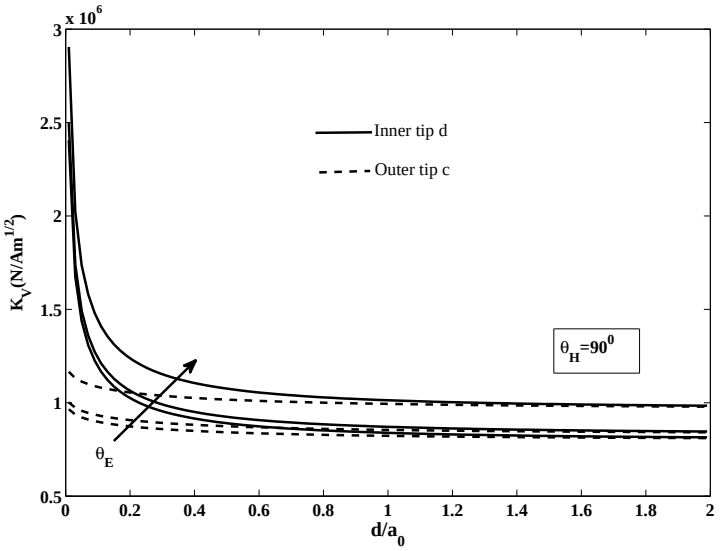

Fig. 10 MIIF versus inter-crack distance for different electric poling with fixed magnetic poling

7.2 Effect of Magnetic poling direction

In this section, the effect of θ_H is shown on the various fracture parameters for fixed $\theta_E = 0^0, 30^0$, and 90^0.

Figs. (11,12,13), Figs. (14,15,16), and Figs. (17,18,19), respectively, show the variations of SIF, EDIF, and MIIF versus inter-crack distance for different θ_H with fixed θ_E. It is observed that K_I, K_{IV} and K_V increases as the fixed θ_E increased from 0^0 to 90^0. Also from the Figs. (11,17), it can be seen that the effect of magnetic poling is negligible over K_I and K_V for fixed $\theta_E = 0^0$.

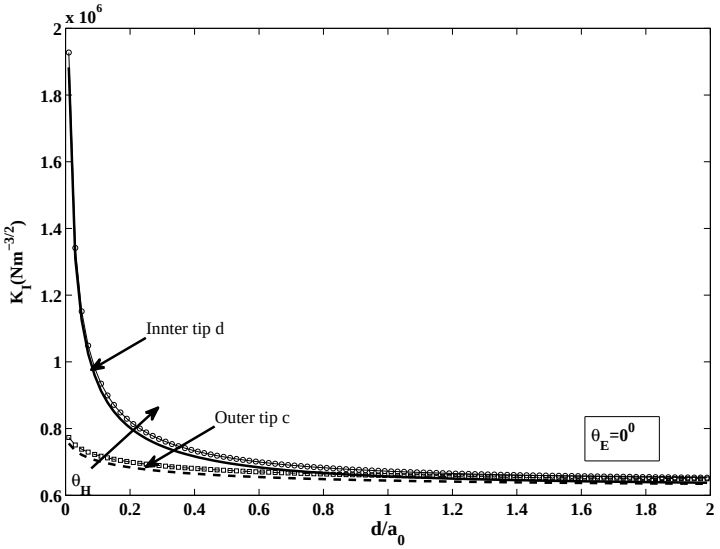

Fig. 11 SIF versus inter-crack distance for different magnetic poling with fixed electric poling

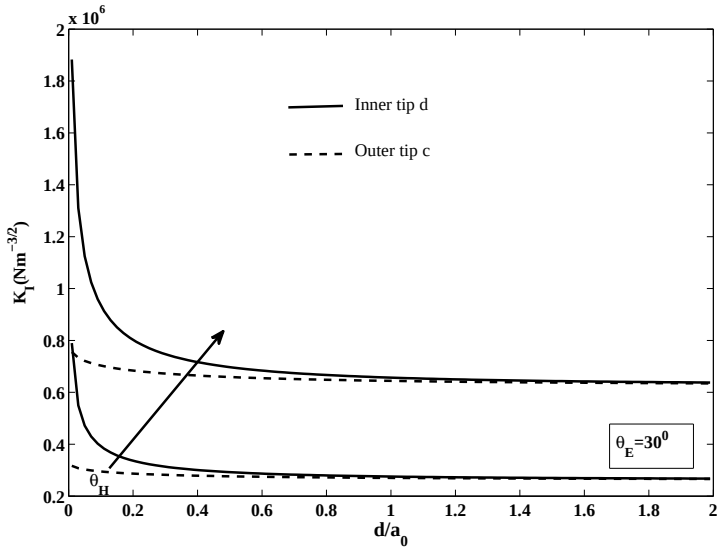

Fig. 12 SIF versus inter-crack distance for different magnetic poling with fixed electric poling

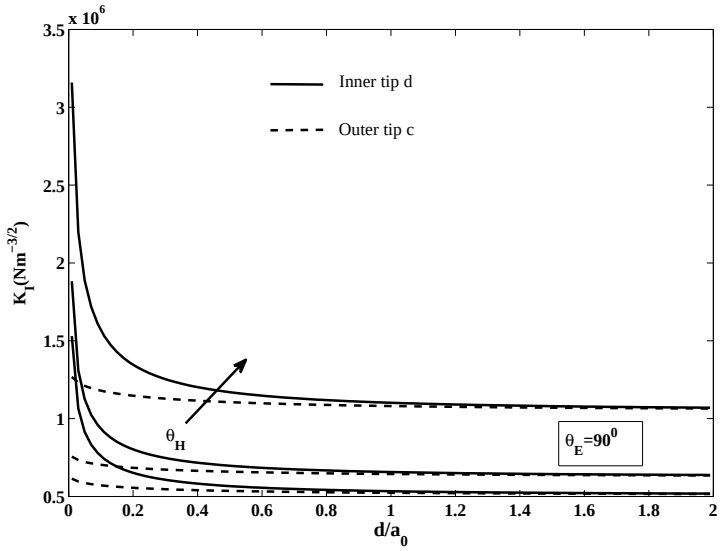

Fig. 13 SIF versus inter-crack distance for different magnetic poling with fixed electric poling

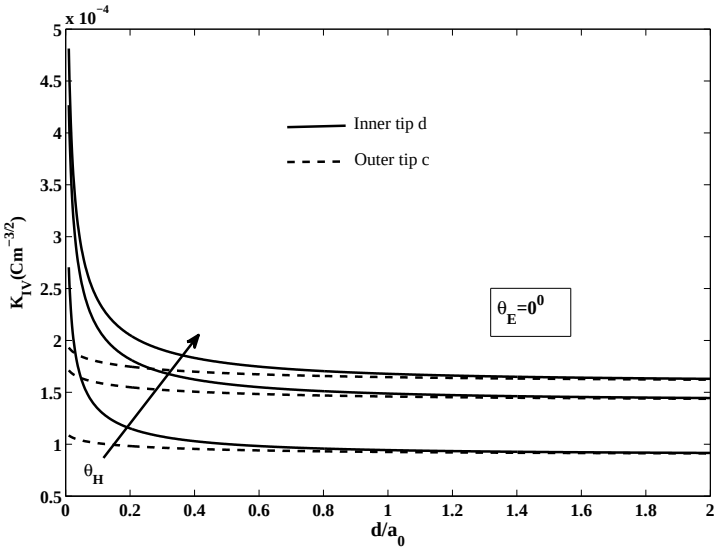

Fig. 14 EDIF versus inter-crack distance for different magnetic poling with fixed electric poling

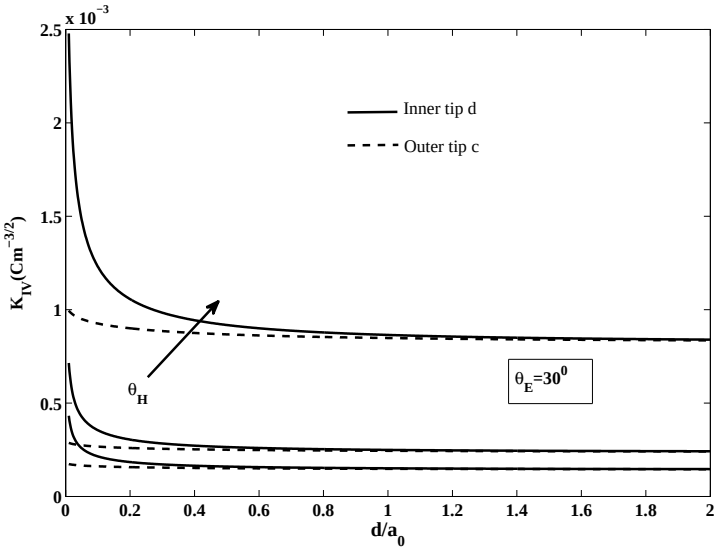

Fig. 15 EDIF versus inter-crack distance for different magnetic poling with fixed electric poling

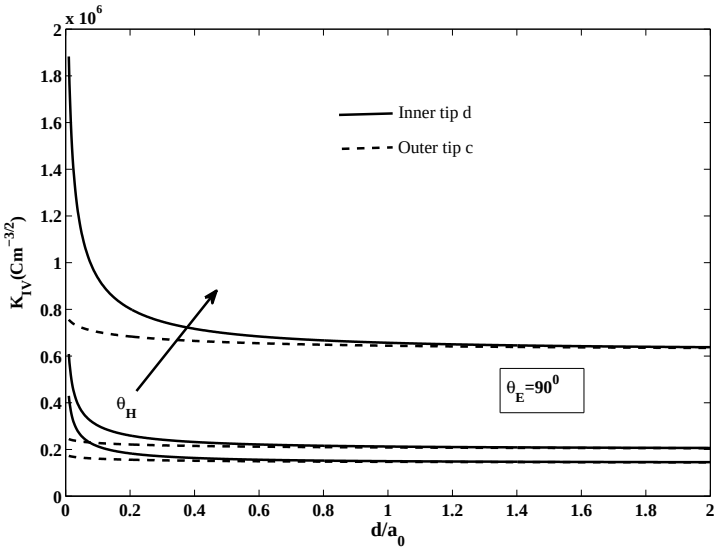

Fig. 16 EDIF versus inter-crack distance for different magnetic poling with fixed electric poling

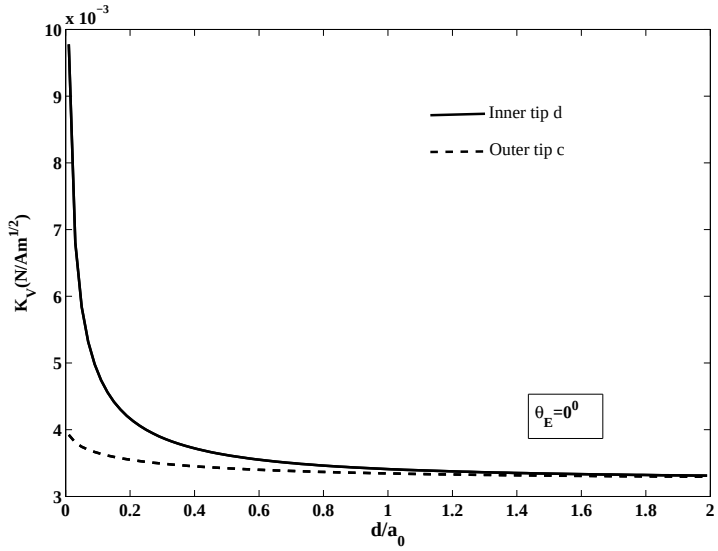

Fig. 17 MIIF versus inter-crack distance for different magnetic poling with fixed electric poling

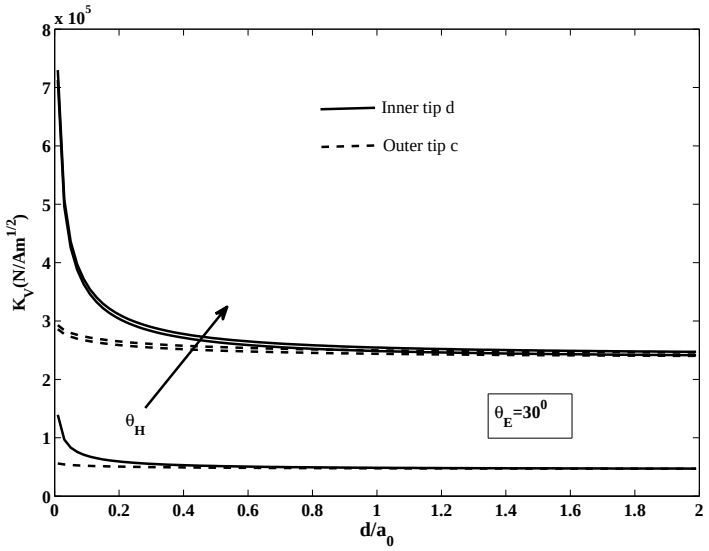

Fig. 18 MIIF versus inter-crack distance for different magnetic poling with fixed electric poling

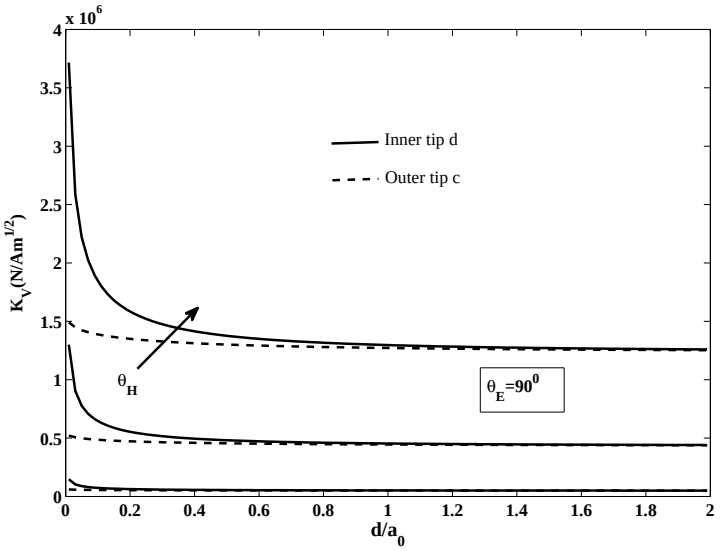

Fig. 19 MIIF versus inter-crack distance for different magnetic poling with fixed electric poling

8 Conclusions

The following conclusions are made from the analytical and numerical studies presented for the proposed two equal collinear semi-permeable cracks model with arbitrarily oriented electric and magnetic poling in MEE media:

- The complex variable methodology is effectively used to model and obtained the analytical solution for two equal collinear semi-permeable cracks weakening MEE media with arbitrarily electric and magnetic

poling directions.

- The closed form analytical expressions are obtained of the SIF, the EDIF, and the MIIF for the proposed problem.
- The effect of electric and magnetic poling direction is graphically shown over the various fracture parameters.
- The numerical investigations of K_1 and K_V demonstrate that the if the electric poling is along the crack line, then magnetic poling does not influence the behaviors of K_1 and K_V.

APPENDIX

Appendix(A)

Consider a composite $BaTiO_3 - CoFe_2O_4$ made of piezoelectric $BaTiO_3$ barium titanate as the inclusions and magnetostrictive $CoFe_2O_4$ cobalt iron oxide as the matrix. The volume fraction of the inclusions is denoted by V_f.

The mixture rule is given by

$$k_{ij}^c = k_{ij}^i V_f + k_{ij}^m (1 - V_f).$$

where the superscripts c, i and m denote the composite, the inclusion, and the matrix. Moreover, k_{ij} stand for the elastic constants c_{ij}, piezoelectric constants e_{ij}, piezomagnetic constants h_{ij}, dielectric permittivity α_{ij} and dielectric permeability γ_{ij}. The above rule is not applicable for the determination of electromagnetic constants, because no electromagnetic coupling is present in any of the single-phase.

Above mixture rule in matrix form can be written as (Sih et al. [7]):

$$\mathbf{M} = \mathbf{M}^B.V_f + \mathbf{M}^C.(1 - V_f)$$

where

$$\mathbf{M}^B = \mathbf{m}_E. \begin{pmatrix} c_{11}^B & c_{13}^B & 0 & 0 & e_{31}^B & 0 & 0 \\ c_{13}^B & c_{33}^B & 0 & 0 & e_{33}^B & 0 & 0 \\ 0 & 0 & c_{44}^B & e_{15}^B & 0 & 0 & 0 \\ 0 & 0 & e_{15}^B & -\alpha_{11}^B & 0 & 0 & 0 \\ e_{31}^B & e_{33}^B & 0 & 0 & -\alpha_{33}^B & 0 & 0 \\ 0 & 0 & 0 & 0 & 0 & -\gamma_{11}^B & 0 \\ 0 & 0 & 0 & 0 & 0 & 0 & -\gamma_{33}^B \end{pmatrix} .\mathbf{m}_E^T$$

and

$$\mathbf{M}^C = \mathbf{m}_H. \begin{pmatrix} c_{11}^C & c_{13}^C & 0 & 0 & 0 & 0 & h_{31}^C \\ c_{13}^C & c_{33}^C & 0 & 0 & 0 & 0 & h_{33}^C \\ 0 & 0 & c_{44}^B & 0 & 0 & h_{15}^C & 0 \\ 0 & 0 & 0 & -\alpha_{11}^C & 0 & 0 & 0 \\ 0 & 0 & 0 & 0 & -\alpha_{33}^C & 0 & 0 \\ 0 & 0 & h_{15}^C & 0 & 0 & -\gamma_{11}^C & 0 \\ h_{31}^C & h_{33}^C & 0 & 0 & 0 & 0 & -\gamma_{33}^C \end{pmatrix} .\mathbf{m}_H^T$$

In above equation, $\mathbf{m}_E$ and $\mathbf{m}_H$ are the coordinate transfer matrix given by

$$\mathbf{m}_E = \begin{pmatrix} \sin^2\theta_E & \cos^2\theta_E & \sin 2\theta_E & 0 & 0 & 0 & 0 \\ \cos^2\theta_E & \sin^2\theta_E & -\sin 2\theta_E & 0 & 0 & 0 & 0 \\ -0.5\sin 2\theta_E & 0.5\sin 2\theta_E & -\cos 2\theta_E & 0 & 0 & 0 & 0 \\ 0 & 0 & 0 & \sin\theta_E & \cos\theta_E & 0 & 0 \\ 0 & 0 & 0 & -\cos\theta_E & \sin\theta_E & 0 & 0 \\ 0 & 0 & 0 & 0 & 0 & \sin\theta_E & \cos\theta_E \\ 0 & 0 & 0 & 0 & 0 & -\cos\theta_E & \sin\theta_E \end{pmatrix}$$

$$\mathbf{m}_H = \begin{pmatrix} \sin^2\theta_H & \cos^2\theta_H & \sin 2\theta_H & 0 & 0 & 0 & 0 \\ \cos^2\theta_H & \sin^2\theta_H & -\sin 2\theta_H & 0 & 0 & 0 & 0 \\ -0.5\sin 2\theta_H & 0.5\sin 2\theta_H & -\cos 2\theta_H & 0 & 0 & 0 & 0 \\ 0 & 0 & 0 & \sin\theta_H & \cos\theta_H & 0 & 0 \\ 0 & 0 & 0 & -\cos\theta_H & \sin\theta_H & 0 & 0 \\ 0 & 0 & 0 & 0 & 0 & \sin\theta_H & \cos\theta_H \\ 0 & 0 & 0 & 0 & 0 & -\cos\theta_H & \sin\theta_H \end{pmatrix}$$

in which θ_H and θ_E are, respectively, the magnetic and electric poling angle as shown in Fig. 1. The superscript B and C stand, respectively, the material constants for $BaTiO_3$ and $CoFe_2O_4$.

Appendix(B)

$$\begin{aligned}
\Pi &= \Upsilon_{22}(\Upsilon_{33}\Upsilon_{44} - \Upsilon_{34}\Upsilon_{43}) + \Upsilon_{23}(\Upsilon_{42}\Upsilon_{34} - \Upsilon_{44}\Upsilon_{32}) + \Upsilon_{24}(\Upsilon_{32}\Upsilon_{43} - \Upsilon_{33}\Upsilon_{42}) \\
\Pi_1 &= \sigma_{33}^{\infty}(\Upsilon_{33}\Upsilon_{44} - \Upsilon_{34}\Upsilon_{43}) - D_3^{\infty}(\Upsilon_{23}\Upsilon_{44} - \Upsilon_{24}\Upsilon_{43}) - B_3^{\infty}(\Upsilon_{24}\Upsilon_{33} - \Upsilon_{23}\Upsilon_{34}) \\
\Pi_2 &= \sigma_{33}^{\infty}(\Upsilon_{32}\Upsilon_{44} - \Upsilon_{34}\Upsilon_{42}) - D_3^{\infty}(\Upsilon_{22}\Upsilon_{44} - \Upsilon_{24}\Upsilon_{42}) - B_3^{\infty}(\Upsilon_{24}\Upsilon_{32} - \Upsilon_{22}\Upsilon_{34}) \\
\Pi_3 &= \sigma_{33}^{\infty}(\Upsilon_{33}\Upsilon_{42} - \Upsilon_{32}\Upsilon_{43}) - D_3^{\infty}(\Upsilon_{23}\Upsilon_{42} - \Upsilon_{22}\Upsilon_{43}) - B_3^{\infty}(\Upsilon_{22}\Upsilon_{33} - \Upsilon_{23}\Upsilon_{32}).
\end{aligned}$$

References

[1] GC Sih, and JZ Zuo(2000). Multiscale behavior of crack initiation and growth in piezoelectric ceramics. *Theor. Appl. Fract. Mech.*, 34:123-141.

[2] GC Sih(2002). A field model interpretation of crack initiation and growth behavior in ferroelectric ceramics: Change of poling direction and boundary condition. *Theor. Appl. Fract. Mech.*, 38:1-14.

[3] LB Sills, Y Motola, and L Shemesh(2008). The M-integral for calculating intensity factors of an impermeable crack in a piezoelectric material. *Eng. Fract. Mech.*, 75:901-925.

[4] Y Motola, LB Sills, and V Fourman(2009). On fracture testing of piezoelectric ceramics. *Int. J. Fract.*, 159:167-190.

[5] K Jangid, and RR Bhargava(2014). A study on influence of poling direction on piezoelectric plate weakened by two collinear semi-permeable cracks. *Acta Mech.*, 225:109-129.

[6] K Jangid, and RR Bhargava(2017). Influence of polarization on two unequal semi-permeable cracks in a piezoelectric media. *Stren. Fract. Complex.*, 10:129-144.

[7] GC Sih, R Jones, and ZF Song(2003). Piezomagnetic and piezoelectric poling effects on mode I and II crack initiation behavior of magnetoelectroelastic materials. *Theor. Appl. Fract. Mech.*, 40:161-186.

[8] GC Sih, and ZF Song(2003). Magnetic and electric poling effects associated with crack growth in $BaTiO_3 - CoFe_2O_4$ composite. *Theor. Appl. Fract. Mech.*, 39: 209-227.

[9] ZF Song, and GC Sih(2003). Crack initiation behavior in magnetoelectroelastic composite under in-plane deformation. *Theor. Appl. Fract. Mech.*, 39:189-207.

[10] K Jangid(2018). Magnetic-saturation zone model for two semipermeable cracks in magneto-electro-elastic medium. *Int. J. Comput. Methd. Eng. Sci. Mech.*, 19:129-137.

[11] AN Stroh(1958). Dislocations and cracks in anisotropic elasticity. *Phil. Mag.*, 30:625-646.

[12] NI Muskhelishvili(1975). *Some Basic Problems of Mathematical Theory of Elasticity*. Noordhoff, Leyden.